Eng. Sci., 2025, **38**, 1837

Engineered Science
DOI: https://dx.doi.org/10.30919/es1837

Research on Cross-Control of Dual-Redundant Starter Motors in Diesel Generators

Feng Qian,[1] Shaokang He,[1] Caixia You,[1,*] Jie Wang,[1] Xiong Bao,[1] Chao Wang,[1] Ruyi Jia,[1] Kaitai Hong,[1] Chen Bai,[2] Kai Wang,[3] Xiaofeng Guo,[4] Timo M. R. Alho[5] and Tao Yu[6]

Abstract

To mitigate potential risks such as starter motor failures and control link malfunctions in the startup control system of emergency backup diesel generators in data centers—risks that may impede the generator's normal startup—this paper proposes a dual-redundant starter motor cross-controller. The controller is designed to enhance the system's fault-tolerance capability and ensure cross-control stability during the startup process. First, based on the PWM (Pulse Width Modulation) input characteristics of dual-redundancy motors, a cross-control strategy is constructed. Second, a dual-redundancy starting motor model is built according to the starting motor type, and fuzzy adaptive PID (Proportional-Integral-Derivative) is used to adjust the motor's output speed. Subsequently, hardware PCB (Printed Circuit Board) and software logic are designed, followed by experimental verification. Results show: under fuzzy PID control, the diesel generator speed (0 to 1500 r/min) has a control accuracy error of 1.33%; under the dual-redundancy strategy, the standby motor switching response time is ⩽ 0.3 seconds with 100% fault recovery success; traditional PID has obvious oscillation and overshoot in the initial 0.02 seconds, while fuzzy PID takes only 0.017 seconds to reach a stable state in motor simulation. This controller significantly improves key performance of dual-redundancy motors, such as starting reliability and control accuracy.

Keywords: Emergency backup diesel generator; Start-up control system; Dual-redundancy start-up motor; Cross-control strategy; Fuzzy control.

Received: 28 August 2025; Revised: 16 October 2025; Accepted: 22 October 2025.
Article type: Research article.

1. Introduction

With the growing global demand for energy and electricity, diesel generators are finding increasingly wide application in scenarios such as engineering construction sites, high-altitude areas with insufficient power supply, as well as in backup power systems for laboratories, computer room servers, data centers, medical facilities, and communication base stations.[1,2] Owing to their stable performance, relatively higher efficiency than other power generation equipment, and strong environmental adaptability, diesel generators have gradually become the preferred choice for backup power sources.[3] Among the components of a diesel generator, its starting control system is the core factor ensuring the generator can initiate normally and operate stably. However, when a single starter motor is used in the starting system, issues such as electrical faults and mechanical wear often occur—these problems not only cause the starting system to fail to initiate properly but may even lead to the shutdown of the entire diesel power generation system.[4] To ensure the normal and stable operation of diesel generator sets, dual starter motors are therefore adopted in their starting systems. Most redundancy

[1] *School of Automobile and Traffic Engineering, Hubei Provincial Engineering Research Center of Advanced Chassis Technology for New Energy Vehicles, Wuhan Scientific and Technological Achievements Transformation Pilot Platform (Base) of Automotive Intelligent Sensor, Wuhan University of Science and Technology, Wuhan, 430065, China*
[2] *The State Key Laboratory of Refractories and Metallurgy, Wuhan University of Science and Technology, Wuhan, 430063, China*
[3] *Cummins Power Generation (China) Co., Ltd, Wuhan, 430056, China*
[4] *LIED UMR 8236, CNRS,Université Paris Cité, Paris, F-75006, France*
[5] *Vaasa University of Applied Sciences, Vaasa, FI-65200, Finland*
[6] *Kangjirun Electromechanical Technology Co.,Ltd., Xiangzhou District, Xiangyang, 441000, China*
**Email:* 2304011@wust.edu.cn (Cx. You)

architectures for dual motors employ a master-slave mode: the main starter motor is in primary operation, while the backup one remains on standby, with automatic switching between the two activated in case of a fault. This master-slave mode, however, fails to fully utilize the backup starter motor; the main motor operates continuously for extended periods, resulting in a higher failure rate and shorter service life.

This study focuses on the diesel generator QSB3.9-G2 and proposes a cross-control design for its dual-redundancy starter motors. The core design concept is based on the master-slave architecture of the starter motors: through the redundant configuration of the two motors, a motor cross-control strategy is developed to eliminate the risk of single-point failure, thereby ensuring the reliable startup and continuous power supply of the diesel generator set in emergency situations.[5] In the traditional diesel generator starting system, the starter motor is a core component, and its failure directly leads to power generation failure. By contrast, the dual-redundancy starter system adopts two sets of independent starting devices (including motors, batteries, and control circuits) and enables automatic switching between the main and backup motors via independent switching logic.[6]

2. Cross timing logic of dual-redundancy start-up motors

For the starting control system of diesel generators, equipping two starter motors cannot fully solve the problems related to the generator's reliable starting and long-term operation. Unordered operation of these two motors will affect the control stability of the system and disrupt the normal operation of the entire diesel power supply system. This study focuses on the starting control of the diesel generator's power supply system (with the starting control system as its core): it proposes a solution that demodulates signals based on the characteristics of the input pulse width modulation (PWM) voltage waveforms of the dual-redundancy starter motors, and conducts timing logic analysis for the motors' cross-control to meet the system's cross-control requirements.[7] The timing logic control table for the start-up motors is shown in Table 1.

(1) The input time and output time of the dual-redundancy starter motors remain synchronized.

(2) The timing logic of the barring input signal controls whether the output signal enables the alternate operation of the primary and secondary starter motors.

(3) The priority determination for the alternate operation of the primary and secondary starter motors is made based on the fault priority level of the primary and secondary starting batteries.

(4) The priority determination for the alternate operation of the primary and secondary starter motors is conducted under the conditions of normal primary/secondary batteries and motor failure.

Among them, symbols are used to denote the specific

Table 1: Timing logic control table for dual-redundancy starter motors.

System state	Drive-by-wheels mode	Master motor input signal	Main motor output signal	Input signal for auxiliary motor	Output signal of auxiliary motor
The battery and motor are in normal operation	Q1	D1	D1		
	Q2			D1	D1
All motors are faulty	Q1	D2	D2	D3	D3
	Q2	D4	D4	D5	D5
The main motor is faulty, and the auxiliary motor is normal	Q1		D6	D7	D1
	Q2			D1	D1
The auxiliary motor is faulty, and the main motor is normal	Q1	D1	D1		
	Q2	D6	D6	D8	D6
Both main and auxiliary batteries are faulty	Q1	D9	D9	D10	D10
	Q2	D11	D11	D9	D9
The main battery is faulty and the auxiliary battery is normal	Q1	D9	D9	D12	D12
	Q2			D1	D1
The main battery is normal and the auxiliary battery is faulty	Q1	D1	D1		
	Q2	D13	D13	D9	D9

meanings of the turning gear mode, main motor input signal, main motor output signal, auxiliary motor input signal, and auxiliary motor output signal respectively.

Q1: Main motor operation;

Q2: Auxiliary motor operation;

D1: a pulse lasting approximately 3 seconds;

D2: three segments with an interval of 15 seconds and a duration of 15 seconds each;

D3:1 second after the main motor stops: two segments with a 45-second interval and a 15-second duration each;

D4:1 second after the auxiliary motor stops: three segments with a 15-second interval and a 15-second duration each;

D5: two segments with a 45-second interval and a 15-second duration each;

D6: one segment with a 15-second interval and a duration of approximately 15 seconds;

D7:15 seconds after the main motor outputs: one segment lasting approximately 3 seconds;

D8:15 seconds after the main motor outputs: one segment with a duration of approximately 3 seconds;

D9: two segments with a 2-second interval and a duration of approximately 2 seconds each;

D10:1 second after the main motor outputs: two segments with a duration of approximately 2 seconds each;

D11:1 second after the auxiliary motor outputs: two segments with a duration of approximately 2 seconds each;

D12:1 second after the main motor outputs: one segment lasting approximately 3 seconds;

D13:1 second after the auxiliary motor outputs: one segment lasting approximately 3 seconds.

Based on the timing logic table for the cross-control of dual-redundancy starter motors, this paper provides a detailed explanation of the timing logic and control principles for two typical control scenarios: 1) normal starting operation with both the main and backup motors available, where the main motor cranks first; and 2) failure of the main starter battery (with the auxiliary starter battery functional), where the backup motor cranks instead of the main motor.

2.1 Normal operation of main and auxiliary motors with main motor cranking first

In the dual-redundancy starter motor system of a diesel generator, the barring operation is one of the indispensable links for startup and a key factor ensuring the normal and stable operation of the startup system.[8] Classified by the barring mode of the starter motor, there are mainly two modes: prime motor first barring and secondary motor first barring. However, the core requirement for the stable operation of the system is to ensure that the input time and output time of the dual-redundancy starter motors remain synchronized. Under the prime motor first barring mode, the PWM signal timing logic for the motor voltage input is shown in Fig. 1. Classified by the barring mode of the starter motor, there are mainly two modes: prime motor first barring and secondary motor first barring. However, the core requirement for the stable operation of the system is to ensure that the input time and output time of the dual-redundancy starter motors remain synchronized. Under the prime motor first barring mode, the PWM signal timing logic for the motor voltage input is shown in Fig. 1.

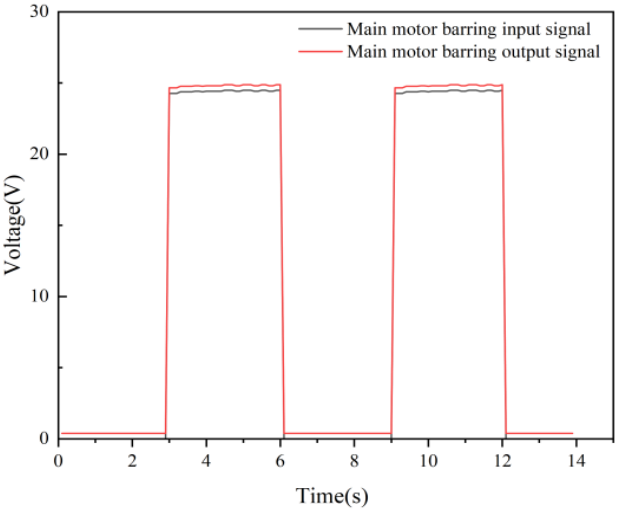

Fig. 1: The timing logic of the PWM signal input by the motor.

The input PWM signal of the main motor appears as a pulse signal lasting approximately 3 seconds. This means that during the startup process of the system, the main motor receives a short excitation signal (about 3 seconds) to trigger its startup and execution of specific operations. Similarly, the output PWM signal of the main motor is also a pulse signal lasting around 3 seconds. This indicates that after the main motor receives the input signal and responds, its output signal remains in an active state for about 3 seconds—this reflects the time characteristics of the main motor from receiving the command to generating the corresponding output. This ensures the timing synchronization between input and output, thereby guaranteeing the normal startup and operation of the main motor. The timing logic for the backup motor's first cranking is identical to that for the main motor's first cranking.

2.2 Both main and auxiliary starting batteries fail with main motor cranking first

To address extreme conditions in the diesel generator starting system and ensure that the starter motors can perform cross-control operation correctly and stably, this study analyzes the

control timing logic of the main motor's first cranking under the condition that the main starting battery fails while the backup starting battery remains functional, as shown in Fig. 2. The main motor generates two 2-second signal segments with a 2-second interval between them, indicating that it attempts cranking in phases at specific time intervals. Approximately 1 second after the start of the main motor's first signal segment, the backup motor generates two 2-second signal segments (with a 2-second interval), meaning it begins cranking attempts at program-scheduled intervals only after the main motor has operated for a certain period.

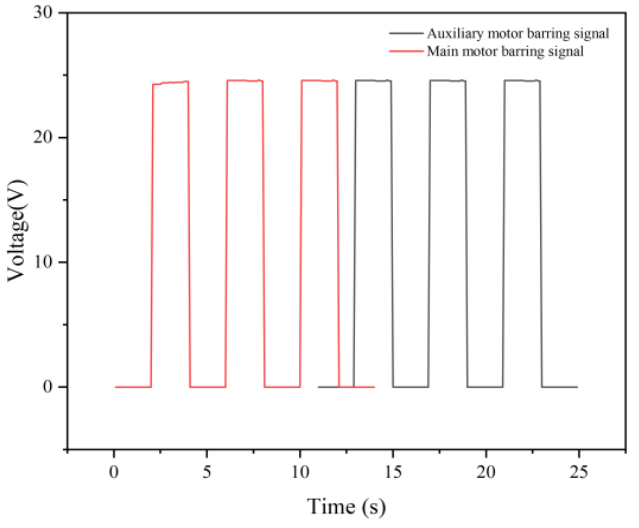

Fig. 2: Start the PWM signal timing logic for the faulty motor voltage input.

The output of the main motor corresponds to its input, presenting two 2-second signal segments with a 2-second interval between them. After receiving the input signal, the main motor outputs power for cranking in accordance with the corresponding timing sequence, and its input and output maintain consistent timing—this ensures the cranking operation proceeds as planned. Approximately 1 second after the start of the main motor's first output signal segment, the backup motor generates two 2-second signal segments (also with a 2-second interval). The backup motor outputs the corresponding cranking power only after the main motor has operated for this 1-second period, and its output timing aligns with its input timing. This sequential timing coordination between the two motors ensures the orderly operation of the dual-redundancy system under fault conditions.

3. Fuzzy proportional-integral-derivative cross-control for dual-redundant starting motors

The adoption of dual-redundancy starter motor control meets the startup adaptability requirements and ensures the stable and reliable operation of the dual-redundancy motors. In this paper, a proportional-integral-derivative (PID) controller based on fuzzy logic is designed to achieve stable speed control of the starter motor.[9] The standard PID controller has a simple structure and strong robustness; however, once its parameters are tuned, they remain fixed. When dealing with nonlinear and time-varying systems, it is difficult for the controller to dynamically adjust its parameters in response to changes in system operation. When the system is subjected to sudden disturbances, the traditional PID controller may exhibit excessively long adjustment times due to fixed parameters, thereby affecting the accuracy and stability of the system. The PID-backstepping hybrid control strategy proposed by Said Ziani et al. integrates the "error correction capability" of PID and the "nonlinear processing capability" of backstepping control to design an adaptive control strategy, realizing low static error, no overshoot, and strong anti-interference control for the speed of Permanent Magnet Synchronous Motors (PMSM). However, its parameter tuning complexity is higher than that of traditional PID, as it also requires tuning the recursive gains of backstepping control. Furthermore, in multi-motor coordinated control scenarios (such as dual-motor synchronous drive), additional cross-error compensation needs to be introduced. Nevertheless, the recursive logic of backstepping control is difficult to directly extend to multi-variable coupled systems, and it is prone to "computational explosion" (where the number of subsystems grows exponentially with the number of variables), making it difficult to meet control requirements.[10]

PID controllers based on fuzzy logic adopt the following algorithm: through the processing flow of "fuzzification → rule reasoning → defuzzification" for input parameters, they dynamically adjust PID parameters to achieve fast response and precise control.[11] Fuzzy PID does not require an accurate mathematical model and can realize adaptive parameter adjustment through fuzzy rules, thus being particularly suitable for complex systems. In this paper, fuzzy PID technology is combined with dual-redundant motor cross-control logic to dynamically adjust the motor startup strategy, so as to meet the real-time control requirements of the diesel generator set startup control system for dual-redundant starter motors.

3.1 Mathematical model of starting motor

Compared with common motors such as stepper motors, direct current (DC) motors, servo motors, and linear motors, brushless DC (BLDC) motors offer advantages including high power density, high efficiency, low noise, and superior speed-torque performance. Ganesh C. J. *et al*. employed the design

of experiments (DOE) and artificial neural networks (ANN) to optimize the stability and smoothness of motor operation.[12] Therefore, they play an increasingly critical role in servo control systems and are widely applied in industrial production and daily life. When establishing the mathematical model of a BLDC motor, it is necessary to integrate its electrical and mechanical characteristics based on motor theory: the mechanical part describes the relationship between rotational speed, torque, and load via a motion equation; the electromagnetic part links current to output torque through an electromagnetic torque equation; and the core of the electrical part relies on a voltage balance equation to quantify its electrical characteristics. Specifically, during the motor's operation, the input voltage of the stator windings must simultaneously overcome resistance losses, inductive energy storage losses, and the back electromotive force (BEMF) generated by the motor's rotation — the mathematical abstraction of this physical process is the voltage balance equation. Compared with other components of the motor's mathematical model, the voltage balance equation serves as a key bridge connecting "input electrical quantities (voltage)" and "internal state quantities (current, back electromotive force)"; its accuracy directly determines how well the model fits the motor's dynamic response, thus making it the primary core component of the motor's mathematical model.[13] The mathematical expression of Eq. (1) is given as follows:

$$V_{abc} = R_s I_{abc} + \omega L_s I_{abc} + e_{abc} \tag{1}$$

where V_{abc} represents the stator phase voltage; R_s represents the stator resistance; L_s represents the stator inductance; I_{abc} represents the stator phase current; ω is the motor angular velocity; e_{abc} is the back - electromotive force constant.

When establishing the mathematical model of a motor, the voltage constraints of the electrical circuit have been described via the voltage balance equation, and the current has been linked with the output torque through the electromagnetic torque equation. Yet the coupling relationship between these two can only be fully expressed with "magnetic flux" as an intermediate variable: the back electromotive force (BEMF) in the voltage balance is essentially a product of changes in magnetic flux, and the generation of electromagnetic torque also depends on the interaction between magnetic flux and current.The flux - linkage balance equation of the motor is in Eqs. (2) and (3):

$$\lambda_r = \psi_r \tag{2}$$

$$\lambda_s = L_s I_{abc} \tag{3}$$

where λ_r is the permanent magnet flux linkage; ψ_r is the permanent magnet magnetic flux; λ_s is the stator flux linkage.

Specifically, the voltage balance equation links the electromagnetic torque via current, while the torque balance equation links the rotational speed via the electromagnetic torque: when the current of motor i changes, the electromagnetic torque changes accordingly, which in turn disturbs the original torque balance, resulting in a change in rotational speed; this change in rotational speed then affects the current through the back electromotive force (BEMF, fed back to the voltage balance equation), forming an "electrical-mechanical" closed loop.The torque balance equation of the motor is in Eq. (4):

$$T_e = k_t(\lambda_r \times \lambda_s) \tag{4}$$

where T_e is the electromagnetic torque; k_t is the torque constant; × denotes the vector cross product.

A simulation model was established in MATLAB to implement the mathematical model of the fuzzy PID controller. The main components of this simulation model include the rotational speed-oriented fuzzy PID controller, power supply, inverter circuit, brushless DC (BLDC) motor, and logic commutation module,[14] as shown in Fig. 3.

3.2 Design of the fuzzy PID controller system

The algorithm realizes real-time optimization of PID parameters by formulating fuzzy rules. Compared with the traditional PID control algorithm, this algorithm can dynamically adjust PID parameters in online mode according to the nonlinearity and time-varying characteristics of the control system. As shown in Fig. 4, this is the fuzzy control logic block diagram for the fuzzy PID controller.[15]

The fuzzy control section of the fuzzy PID controller takes two input variables: the error between the reference motor speed (calibrated speed) and the actual feedback speed, and the rate of change of this speed error. Fuzzification is performed in the fuzzy rule base based on fuzzy PID control logic. For these input variables, the universe of discourse for the speed error is [-3, 3], and that for the speed error rate is also [-3, 3]. The proportional, integral, and differential (PID) terms are defined as the output variables. A fuzzy rule control table is constructed, with the speed error as the columns and the speed error rate as the rows of the tables.[16]

$$E = \{ NB, NM, NS, ZO, PS, PM, PB \} \tag{5}$$

The fuzzy subsets in Eq. (5) representing the input variables are as follows: NB denotes Negative Big, NM denotes Negative Medium, NS denotes Negative Small, ZE denotes Zero, PS denotes Positive Small, PM denotes Positive Medium, and PB denotes Positive Big. The fuzzy PID control rules are presented in Table 2.

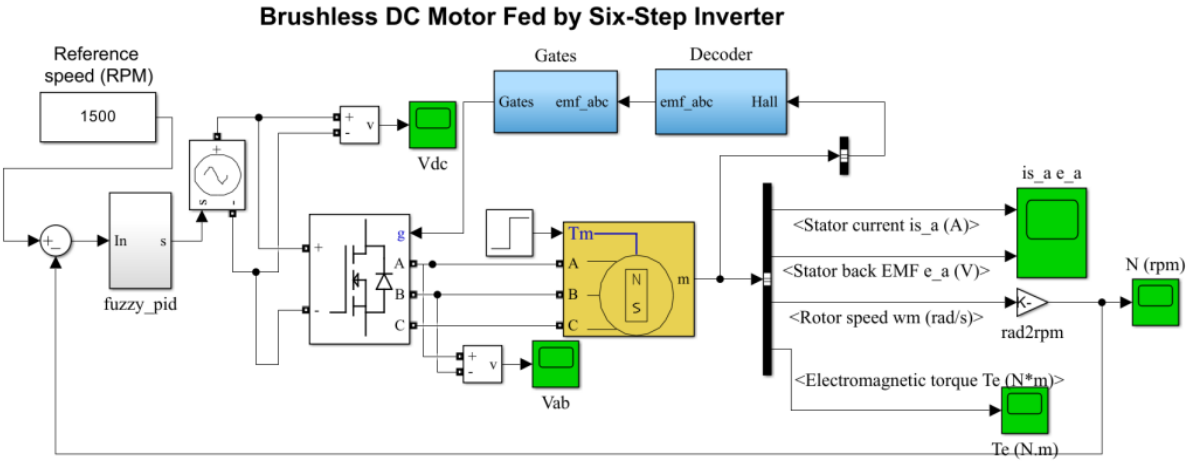

Fig. 3: Fuzzy PID simulation model of BLDC motor.

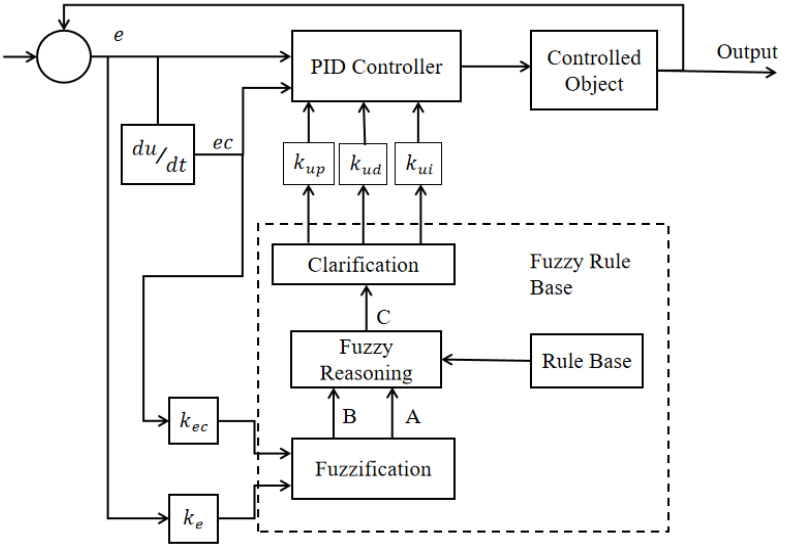

Fig. 4: Fuzzy PID controller fuzzy control logic block diagram.

Table 2: Fuzzy PID - K_p, K_i, K_d control rules.

Parameter	Core control logic	
K_p	Large error stage（e = NB/NM）: The deviation seriously deviates from the target	If ec is negative → increase (quickly reduce the error); If ec is positive → decrease (prevent overshoot).
	Medium error (e = NS): The deviation is close to the target	Take an intermediate value to balance response speed and stability.
	Small error (e = ZO/PS/PM/PB)	Decrease to avoid overshoot affecting accuracy.
K_i	Large error stage（e = NB/NM）: The deviation seriously deviates from the target	Decrease to prevent large overshoot caused by "integral saturation".
	Medium error （e = NS）: The deviation is close to the target	Gradually transition to balance "error elimination demand" and "overshoot risk".
	Small error (e = ZO/PS/PM/PB)	Increase to strengthen the integral effect and eliminate steady-state error.
K_d	When e or ec is large ((e = NB/NM) and (ec = PB), where the deviation is large and changes rapidly)	Ncrease to suppress overshoot caused by sudden error changes.
	When e and ec are small (the deviation is small and changes gently)	Decrease to avoid excessive damping leading to slow response and ensure system smoothness.

The fuzzy inference engine is used to perform fuzzy reasoning on the input variables. After fuzzy reasoning is completed, defuzzification is performed to convert the fuzzy output into precise adjustments of PID parameters. According to the classification of 7 fuzzy subsets in the fuzzy rules, the universe of discourse is equally divided into 7 fuzzy centers, and the coverage width of each fuzzy set is defined based on the input range.[17] In this paper, a triangular membership function is employed for defuzzification. For each fuzzy set (such as NB, NM, *etc*.), the distance from the input value to the center is calculated and converted into a membership degree using Eq. (6).

$$f(x) = 1 - \frac{x-c}{w} \tag{6}$$

where c represents the center value of the fuzzy set, and w is the width parameter. When x lies within the interval [c-w, c+w], the membership degree assumes a non-zero value; otherwise, it is zero. The width parameter w is set to 1 based on the motor's performance parameters. The triangular membership function can be expressed as follows. In Eq. (6), x denotes the input parameter variable. Using this triangular membership function, the defuzzification operation is performed to compute the membership degree of the input parameter for each fuzzy subset.[18] Subsequently, the centroid method is employed for defuzzification, which is defined as Eq. (7):

$$\begin{cases} K_p = \Delta K_p + K_p' \\ K_I = \Delta K_I + K_I' \\ K_D = \Delta K_D + K_D' \end{cases} \tag{7}$$

The output of fuzzy PID controller is expressed as follows Eq. (8):

$$E(t) = K_p e(t) + K_I \int e\,(t)dt + K_D \frac{de(t)}{dt} \tag{8}$$

Through tuning the fuzzy PID rules for the starter motor speed, fuzzy rules are constructed in the MATLAB simulation model. As shown in Fig. 5, the fuzzy PID logic simulation takes the difference between the actual speed and the calibrated speed as a reference. The fuzzy rule controller is applied to dynamically adjust the parameter values of K_p, K_I, and K_D in the PID controller.[19]

4. Hardware and software design and experimental simulation of dual-redundancy starter motor

4.1 Hardware control design of dual-redundancy motor

For the hardware control board design of the dual-redundancy starter motor, a PWM signal detection module is required to detect the PWM signal input to the diesel generator starting system. The main control chip interprets and processes the received PWM signal, and finally outputs control signals through the chip's General Purpose Input/Output (GPIO) ports to control the operation of the dual-redundancy starter motor. This paper elaborates on the design from four aspects: the power supply module, the main control module, the RS232 communication module, and the optocoupler drive module.

The power supply module is primarily responsible for providing stable voltage and current input to the entire hardware circuit system.[20] In this design, the TPS54360 series switching regulator chips are adopted, as shown in Fig. 6 (Power Supply Module Circuit). This series of switching regulator chips can significantly reduce power loss between input and output voltages. The output voltage is regulated by adjusting the resistance value of the feedback resistor at the

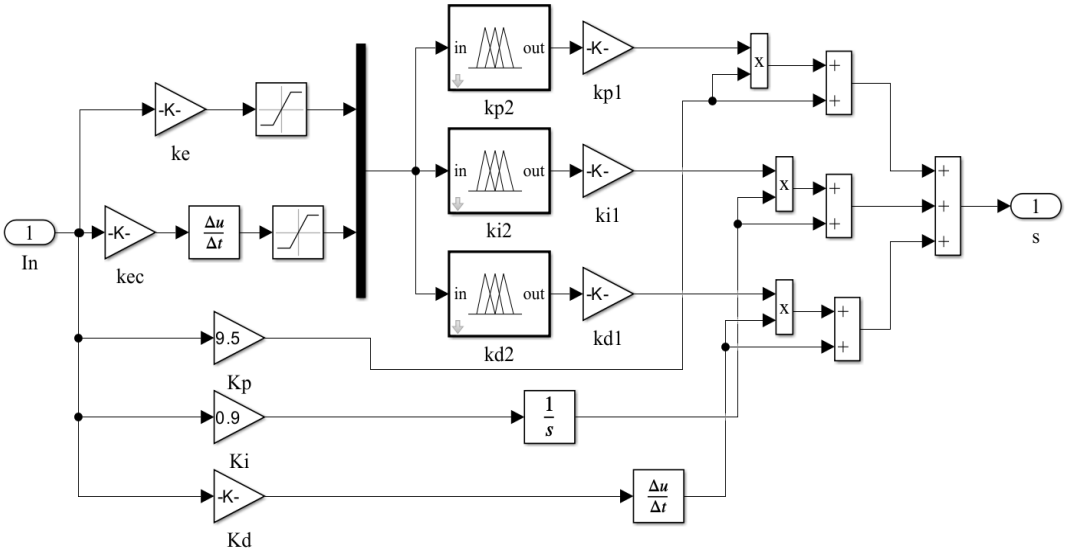

Fig. 5: MATLAB SIMULINK fuzzy PID logical rules simulation model.

FB port of the switching regulator chip. Specifically, the input 24V DC voltage is first stepped down to 5V through the switching regulator chip; then, the Buck Converter (BUCK) voltage regulator chip further steps down the 5V to 3.3V by adjusting the resistance ratio via the Adjust Pin (ADJ) port. This design meets the requirements of a stable voltage fluctuation range and low power loss, thereby providing stable voltage and current for the hardware circuit.

The primary objective of the RS232 communication module design is to enable interaction with the host computer, enabling the input and output of control signals and data via the RS232 communication interface.[21] This allows for real-time data monitoring and seamless data transmission through hardware-software interaction. In this paper, the SP3232EEY series communication chip is employed for circuit implementation, as illustrated in Fig. 7 (RS232 Communication Module Circuit). Communication with the host computer is established through the T1IN and R1OUT signal lines. The D-DMS009PF series communication female connector is utilized to ensure the stability of communication signal quality. Additionally, a bidirectional voltage regulator diode PESD5VL2BT.215 is integrated to filter out clutter interference, safeguarding the integrity and stability of signal transmission.

The optocoupler drive module is designed to achieve signal transmission utilizing the high-speed signal transfer characteristics of optocouplers, thereby controlling the transmission of dual-redundancy motor control signals via GPIO. In this design, the GAQY252G3S optocoupler isolation chip is employed, which prevents mutual interference between input and output signals and provides excellent photoelectric isolation performance. As shown in Fig. 8 (Optocoupler Drive Module Circuit), the high or low voltage level of the Sub_Signal input signal regulates the brightness of the light-emitting diode within the optocoupler isolation chip. This, in turn, controls the turn-on and turn-off of the field-effect transistor (FET), ultimately determining the high or low level of the Sub_Signal_MCU output signal.

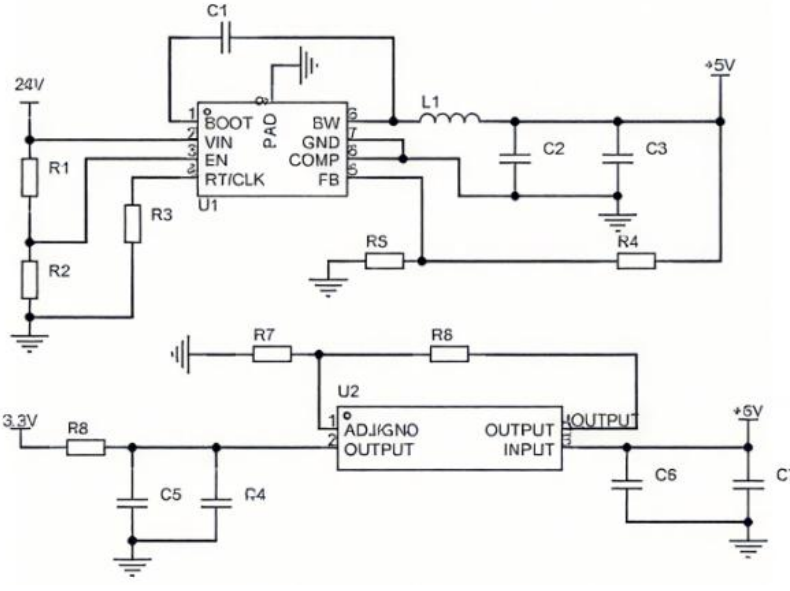

Fig. 6: Power module circuit.

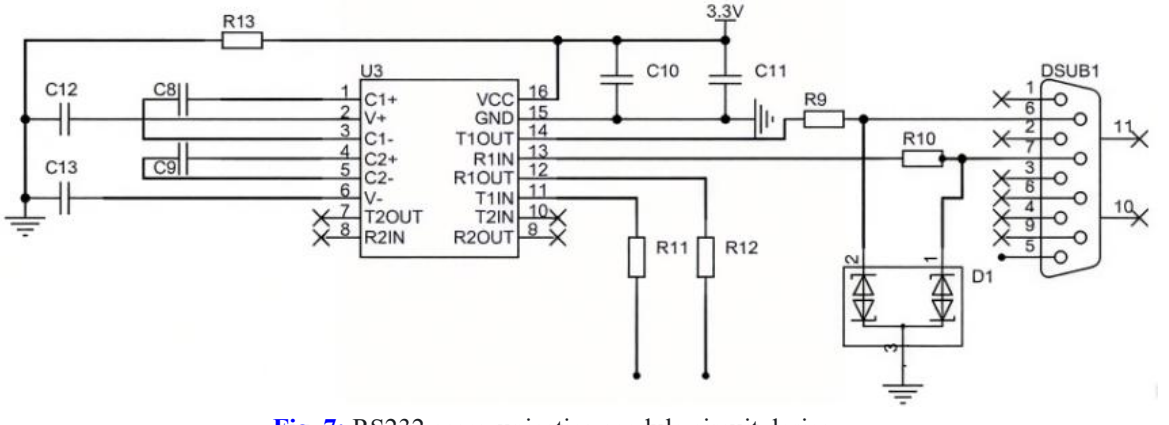

Fig. 7: RS232 communication module circuit design.

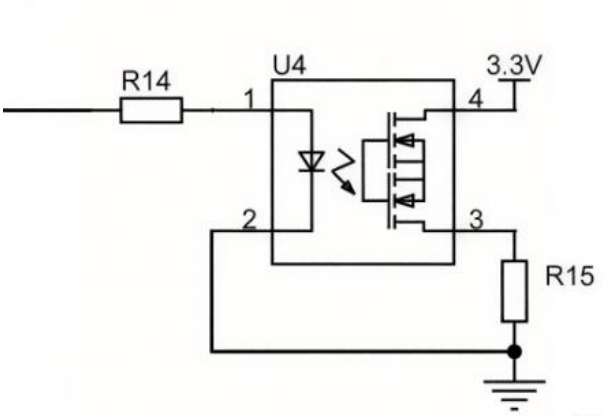

Fig. 8: Optocoupler drive module circuit design.

The main control module is designed to handle complex cross-logic control. In this paper, the STM32F4 series chips are selected for circuit design. This series of chips integrates high performance, real-time processing performance, digital signal processing, low power consumption, low-voltage operation, and interconnectivity. As shown in Fig. 9, it has a wealth of peripheral interfaces such as GPIO (General Purpose Input/Output), I2C (Inter-Integrated Circuit), SPI (Serial Peripheral Interface), ADC (Analog-to-Digital Converter), CAN (Controller Area Network), and USART (Universal Synchronous/Asynchronous Receiver/Transmitter), with a working frequency of up to 180MHz, excellent processing performance, low dynamic power consumption, and strong capability for complex operations. Meanwhile, the STM32F4 series chips feature faster analog-to-digital conversion speed, lower ADC/DAC operating voltage, 32-bit timers, a real-time clock (RTC) with a calendar function, significantly enhanced I/O multiplexing function, 4K bytes of battery-backed SRAM (Static Random-Access Memory), and faster USART and SPI communication speeds. These characteristics meet the requirements for data sampling of the motor input PWM and real-time communication with the host computer.

4.2 Software control design of dual-redundancy motor software program

Software programming is crucial to ensuring that the entire hardware circuit can automatically operate according to design intentions. By writing corresponding programs, we carry out software development and design for dual-redundancy motors to realize cross-logic control of the dual motors. The core program of the control system software is the foundation of the system, specifying its operational process and overall structure. Its main operational process includes initializing the Microcontroller Unit (MCU), which involves adjusting settings of internal devices such as serial ports, timers, and registers. The flowchart of the main program is shown in Fig. 10.

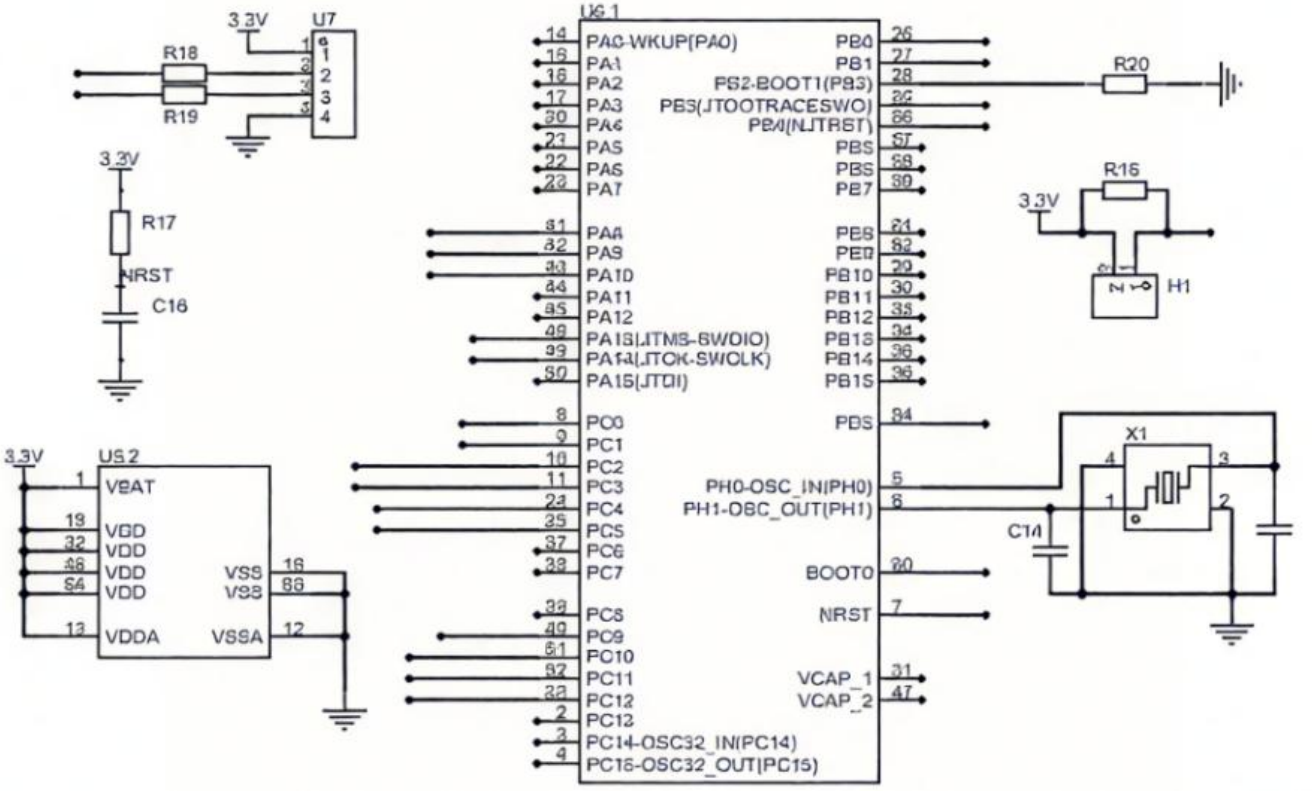

Fig. 9: Master control module circuit design.

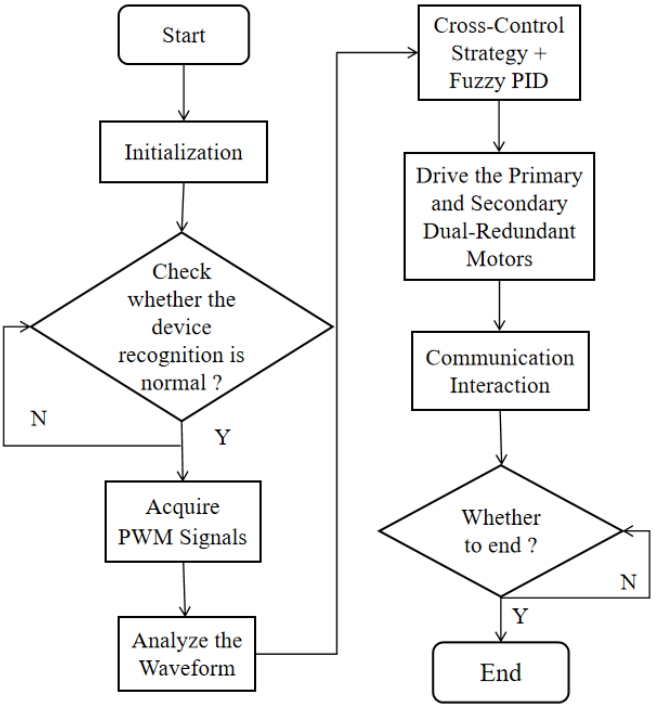

Fig. 10: Master program flow chart.

The main operation process of the program includes:

(1) Completing the initialization of the MCU, including adjusting internal device settings. Then, it is necessary to check the external devices of the system to verify their normal operating status; after the hardware devices are detected and confirmed to be in normal working condition, communication with the host computer will be established.

(2) After the initialization and hardware inspection are completed, the PWM detection module will collect the signals transmitted by the motor in real-time and send them to the main control module. Subsequently, the main control module receives the input data and executes the corresponding fuzzy PID motor control algorithm program. thereby achieving accurate control of the dual-redundancy motors.

(3) After completing the motor control, communication with the host computer's communication assistant is performed to transmit relevant motor control data to the host computer for display.

5. Experimental simulation of dual-redundancy starter motor

To verify the feasibility and reliability of the cross-control logic for dual-redundancy motors, experimental tests were conducted on the diesel generator system based on the cross-control logic principle of dual-redundancy motors.[22] According to the typical control operating conditions mentioned above, experiments were carried out respectively for two scenarios: normal operation of main and auxiliary motors with the main motor cranking first, and main battery failure with normal auxiliary battery and the main motor cranking first.

The output timing sequence of the primary and secondary motors under normal operation is shown in Fig. 11. After the primary motor starts, its output terminal continuously generates a high-level logic signal for 3 seconds to control the primary motor for power output. Under this cross-control logic, the starting battery maintains a normal operating state, with the voltage stabilized at 24V. When the primary motor is in the output state, the voltage of the primary battery fluctuates slightly; during this period, the motor speed is maintained at 1500 r/min, with the actual lower limit deviation of the motor speed being 1480 r/min and the upper limit deviation being 1510 r/min, resulting in a control accuracy of approximately ±1.33%. Startup transient experiments show that under fuzzy PID control, the rise time (response time) for the diesel generator speed to increase from 0 to the target value of 1500 r/min is 0.8s; in contrast, the response time of traditional PID control is 1.5s. The response speed of the starter motor is improved by 46.7%, ensuring that the diesel generator meets the specified starting speed requirement.

Fuzzy PID is based on an "error-error rate of change" rule base and can quickly adjust parameters during the startup transient, which exactly matches the diesel generator's requirement of "fast startup while avoiding engine wear caused by speed overshoot". Under the normal startup test condition: For the traditional PID, the control accuracy error

of the starter motor speed is ±3.33%, the response time is more than 1s, and the steady-state speed fluctuation of the motor is ±30 r/min. For the fuzzy PID, the control accuracy error of the starter motor speed is approximately ±1.33%, the response time is less than 1s, and the steady-state speed fluctuation of the motor is ±10 r/min. Experimental results indicate that under normal operating conditions, the dual-redundancy motor control system can stably drive the primary motor to complete startup while maintaining sufficient voltage stability and speed, fully meeting the starting requirements of the diesel generator.

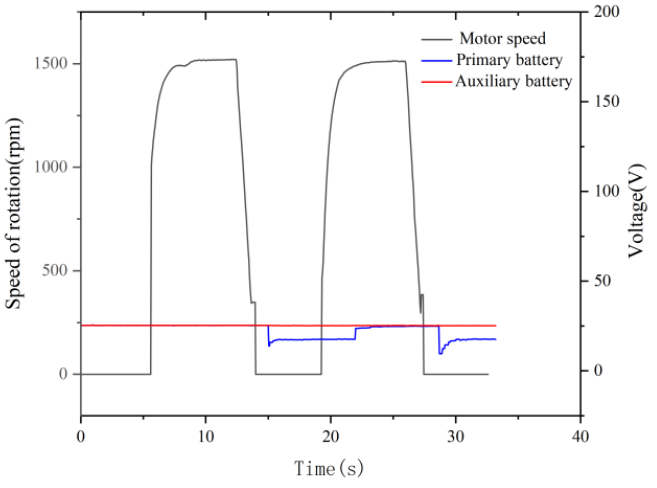

Fig. 11: Normal motor the main motor first turns the wheel to output the timing.

The timing logic for the scenario where both the main and auxiliary starter batteries fail and the main motor cranks first is shown in Fig. 12. It indicates that when both starter batteries fail during main motor cranking, the system attempts to drive the main motor with 3 cycles of 2-second PWM power outputs. After a 1-second interval, the auxiliary motor similarly delivers 3 cycles of 2-second PWM power outputs. Due to the failure of the starter batteries, the motor speed remains at a low level of 150 rpm, failing to start the diesel generator for normal power supply.

Primary motor fault simulation experiment (30 repeated tests): When a sudden electrical fault occurs in the primary motor, the switching response time of the backup motor under the dual-redundancy control strategy is ≤ 0.3s, with a fault recovery success rate of 100%. During the switching process, the speed fluctuation is ≤ ± 5 r/min, and no diesel generator startup interruption occurred. In contrast, under the same fault conditions, the traditional single-motor architecture had a startup failure rate of 15% (4 out of 30 tests), and the average recovery time exceeded 5s.

In the dual-redundancy motor startup experiment, the setpoint of the motor speed signal was adjusted to 1500 rpm, and the comparison diagram of motor output speeds is shown in Fig. 13. The traditional PID algorithm exhibited obvious oscillations and overshoot within the first 0.02 seconds, indicating that the PID algorithm caused unstable speed regulation responses, which negatively affected the control effect. In contrast, the fuzzy PID algorithm reached a stable state within 0.017 seconds without significant oscillations or overshoot in the motor speed simulation, demonstrating a faster response. Compared with the traditional PID algorithm, the fuzzy PID control effect is significantly better, with stable output. It can be concluded that the fuzzy PID designed in this paper outperforms the traditional PID in motor speed control, exhibiting excellent dynamic response and robustness in practical applications.[23]

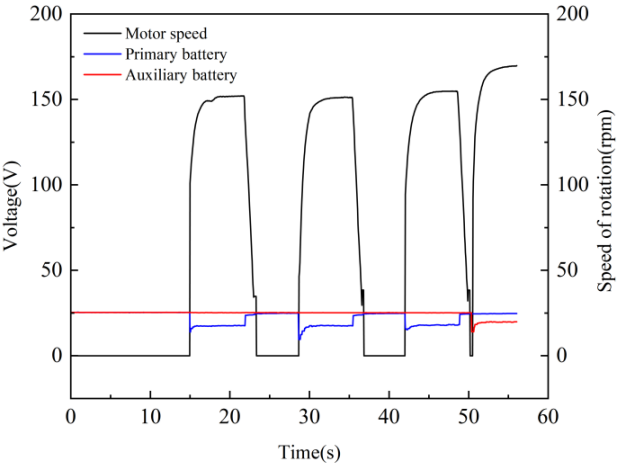

Fig. 12: Start the timing logic when all batteries are faulty and the main motor first turns the car.

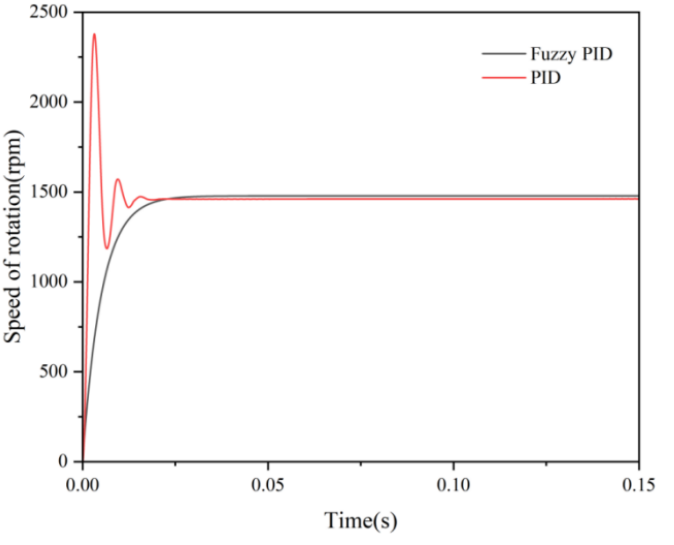

Fig. 13: Fuzzy PID speed simulation control of brushless motor in MATLAB.

6. Conclusion

In the emergency standby diesel power supply system of data centers, the start control module may cause emergency power outages due to electrical faults, single-motor operation, or overload, leading to data center paralysis.[24] This study adopts a master-slave architecture to implement a dual-redundancy motor control scheme. By collecting PWM timing voltage logic signals at the start motor input and analyzing the status of the start battery and motor, a dual-redundancy motor control strategy is designed. Based on differences in motor start timing logic, this strategy achieves dynamic adjustment for real-time switching between the main and standby motors in the diesel generator start control system. Compared with the single-motor architecture in existing data center diesel systems, the dual-redundancy design in this study eliminates single-point faults and improves fault tolerance.[25] This fully aligns with the "zero-interruption emergency power supply for data centers" industry standard proposed by the International Energy Agency (IEA, 2024).

Experiments show that compared with traditional PID control, fuzzy PID control enables faster and more accurate speed regulation, meeting the minimum start speed requirement of diesel generators and ensuring stable output power—consistent with the theoretical expectation of fuzzy PID in nonlinear and time-varying systems (Wang et al., 2021). This study combines dual-motor redundancy control logic with the fuzzy PID algorithm: it not only avoids startup faults of single-architecture start motors but also addresses the limitations of traditional single-architecture start motors and the rigidity of main-standby dual-motor operation in dual-redundancy architectures (*i.e.*, the standby start motor is activated only when the main motor fails). Additionally, it achieves faster and more precise speed regulation. In the simulation experiments of PID and fuzzy PID control in this study, the stability and reliability of fuzzy PID in motor speed control are evident, which meets the minimum start speed requirement of diesel generators and ensures stable power output.

Acknowledgments

This study was funded by the Hubei Provincial Central Committee to Guide Local Science and Technology Development Project (No. 2025EIA020).

Conflict of Interest

There is no conflict of interest.

Supporting Information

Not applicable.

CRediT Statement

Feng Qian: Writing – review & editing, Supervision, Resources, Project administration, Investigation, Funding acquisition. **Shaokang He**: Writing – Original draft, Methodology, Investigation, Formal analysis, Data curation. **Caixia You**: Supervision, Resources,Project administration. **Jie Wang**: Supervision, Resources,Project administration. **Xiong Bao**: Supervision, Resources, Project administration. **Chao Wang**: Supervision, Resources. **Ruyi Jia**: Supervision, Resources,Data curation. **Kaitai Hong**: Supervision, Resources,Data curation. **Chen Bai:** Supervision, Resources. **Kai Wang**: Supervision, Resources, Funding acquisition. **Xiaofeng Guo**: Supervision, Resources. **Timo M. R. Alho**: Supervision, Resources. **Tao Yu**: Supervision, Resources.

References

[1] J. Hamilton, M. Negnevitsky, X. Wang, E. Semshchikov, The role of low-load diesel in improved renewable hosting capacity within isolated power systems, *Energies*, 2020, **13**, 4053, doi: 10.3390/en13164053.

[2] J. Marqusee, D. Jenket, Reliability of emergency and standby diesel generators: Impact on energy resiliency solutions, *Applied Energy*, 2020, **268**, 114918, doi: 10.1016/j.apenergy.2020.114918.

[3] A. K. Jain, S. Mathapati, V. T. Ranganathan, V. Narayanan, Integrated starter generator for 42-V powernet using induction machine and direct torque control technique, *IEEE Transactions on Power Electronics*, 2006, **21**, 701-710, doi: 10.1109/TPEL.2006.872364.

[4] L. Sun, X. Li, L. Chen, H. Shi, Z. Jiang, Dual-motor coordination for high-quality servo with transmission backlash, *IEEE Transactions on Industrial Electronics*, 2023, **70**, 1182-1196, doi: 10.1109/TIE.2022.3156154.

[5] Z. Li, K. T. Wang, J. S. Wang, Z. H. Zhang, X. Q. Guo, H. X. Sun, Cross-coupling control strategy based on intelligent adaptive control for cross-shaped dual-axis linear motors, *IET Electric Power Applications*, 2023, **17**, 1212-1224, doi: 10.1049/elp2.12336.

[6] H. Guo, X. He, J. Xu, W. Tian, G. Sun, L. Ju, D. Li, Design of an aviation dual-three-phase high-power high-speed permanent magnet assisted synchronous reluctance starter-generator with antishort-circuit ability, *IEEE Transactions on Power Electronics*, 2022, **37**, 12619-12635, doi: 10.1109/TPEL.2022.3172339.

[7] W. Bu, S. Guo, Z. Fan, J. Li, Improved adaptive PI-like fuzzy control strategy of permanent magnet synchronous motor, *Energies*, 2025, **18**, 362, doi: 10.3390/en18020362.

[8] F. Jiang, C. Tu, Q. Guo, Z. Wu, Y. Li, Adaptive soft starter for a three-phase induction-motor driving device using a multifunctional series compensator, *IET Electric Power Applications*, 2019, **13**, 977-983, doi: 10.1049/iet-epa.2018.5079.

[9] H. H. Choi, H. M. Yun, Y. Kim, Implementation of evolutionary fuzzy PID speed controller for PM synchronous motor, *IEEE Transactions on Industrial Informatics*, 2015, **11**, 540-547, doi: 10.1109/TII.2013.2284561.
[10] S. Ziani, S. Essahel, Y. A. Zorgani, M. Elghmary, Control of permanent magnet synchronous motor by integrating the proportional - integral - derivative - regulation with backstepping, *ES Energy & Environment*, 2023, **21**, 842, doi: 10.30919/esee8c842.
[11] Y. Luo, T. Jin, X. Li, X. Qin, Y. Han, Research on pump speed control system based on fuzzy PID, *Mechanics*, 2023, **29**, 225-234, doi: 10.5755/j02.mech.32721.
[12] C. J Ganesh, G. S. Vijay, I. B. Siddappa, Modelling of interior permanent magnet motor and optimization of its torque ripple and cogging torque based on design of experiments and artificial neural networks, *Engineered Science*, 2022, **18**, 193-203, doi: 10.30919/es8d677.
[13] K. Premkumar, B. V. Manikandan, Fuzzy PID supervised online ANFIS based speed controller for brushless DC motor, *Neurocomputing*, 2015, **157**, 76-90, doi: 10.1016/j.neucom.2015.01.032.
[14] H. Yin, W. Yi, J. Wu, K. Wang, J. Guan, Adaptive fuzzy neural network PID algorithm for BLDCM speed control system, *Mathematics*, 2022, **10**, 118, doi: 10.3390/math10010118.
[15] M. Çunkas, O. Aydoğdu, Realization of fuzzy logic controlled brushless DC motor drives using Matlab/Simulink, *Mathematical and Computational Applications*, 2010, **15**, 218-229, doi: 10.3390/mca15020218.
[16] H. Li, L. Zhang, K. Cai, G. Chen, An improved robust fuzzy-PID controller with optimal fuzzy reasoning, *IEEE Transactions on Systems, Man, and Cybernetics, Part B (Cybernetics)*, 2005, **35**, 1283-1294, doi: 10.1109/TSMCB.2005.851538.
[17] T. Wu, Y. Jiang, Y. Su, W. Yeh, Using simplified swarm optimization on multiloop fuzzy PID controller tuning design for flow and temperature control system, *Applied Sciences*, 2020, **10**, 8472, doi: 10.3390/app10238472.
[18] K. Premkumar, B. V. Manikandan, Adaptive Neuro-Fuzzy Inference System based speed controller for brushless DC motor, *Neurocomputing*, 2014, **138**, 260-270, doi: 10.1016/j.neucom.2014.01.038.
[19] I. Cukdar, T. Yigit, H. Celik, Balance control of brushless direct current motor driven two-rotor UAV, *Applied Sciences*, 2024, **14**, 4059, doi: 10.3390/app14104059.
[20] S. Han, Y. Wang, Z. Xie, Y. Guan, J. M. Alonso, D. Xu, Continuously adjustable modular bidirectional switched-capacitor DC–DC converter, *IEEE Transactions on Power Electronics*, 2022, **37**, 12944-12948, doi: 10.1109/TPEL.2022.3181495.
[21] L. Qian, K. Gu, Y. Fu, Y. Shen, S. Xu, A wireless ad hoc network communication platform and data transmission strategies for multi-bus instruments, *Electronics*, 2024, **13**, 3596, doi: 10.3390/electronics13183596.
[22] K. Wang, B. Qu, M. Gao, Redundancy control strategy for a dual-redundancy steer-by-wire system, *Actuators*, 2024, **13**, 378, doi: 10.3390/act13090378.
[23] C. Chao, N. Sutarna, J. Chiou, C. Wang, Equivalence between fuzzy PID controllers and conventional PID controllers, *Applied Sciences*, 2017, **7**, 513, doi: 10.3390/app7060513.
[24] S. Hasan, N. Gurung, K. M. Muttaqi, S. Kamalasadan, Electromagnetic field-based control of distributed generator units to mitigate motor starting voltage dips in power grids, *IEEE Transactions on Applied Superconductivity*, 2019, **29**, 0602604, doi: 10.1109/TASC.2019.2895468.
[25] M. S. Scioletti, A. M. Newman, J. K. Goodman, A. J. Zolan, S. Leyffer, Optimal design and dispatch of a system of diesel generators, photovoltaics and batteries for remote locations, *Optimization and Engineering*, 2017, **18**, 755-792, doi: 10.1007/s11081-017-9355-4.